

## Supporting Information

### **KCl-CaCO<sub>3</sub> nanoclusters armored with Pt Nanocrystals for Enhanced Electro-driven Tumor Inhibition**

Tong Chen,<sup>a</sup> Yike Fu,<sup>\*,b</sup> Ruoyu Zhang,<sup>\*,c</sup> Gaorong Han,<sup>a</sup> and Xiang Li,<sup>\*,a, b</sup>

<sup>a</sup> State Key Laboratory of Silicon Materials, School of Materials Science and Engineering, Zhejiang University, Hangzhou, Zhejiang 310027, People's Republic of China.

<sup>b</sup> ZJU-Hangzhou Global Scientific and Technological Innovation Centre, Zhejiang University, Hangzhou, 311200, P.R. China.

<sup>c</sup> Department of Geriatrics, The Second Affiliated Hospital, School of Medicine, Zhejiang University, Hangzhou 310009, P.R. China.

\* Corresponding Authors: Dr Xiang Li, E-mail: [xiang.li@zju.edu.cn](mailto:xiang.li@zju.edu.cn); Dr Yike Fu, E-mail: [fyk3927@zju.edu.cn](mailto:fyk3927@zju.edu.cn); Dr Ruoyu Zhang, E-mail: [zhangruoyu@zju.edu.cn](mailto:zhangruoyu@zju.edu.cn).

## Materials

Calcium chloride dihydrate ( $\text{CaCl}_2 \cdot 2\text{H}_2\text{O}$ ), poly(maleicanhydride-alt-1-octadecene) ( $\text{C}_{18}\text{PMH}$ ), mPEG-NH<sub>2</sub> (5k), 1-ethyl-3-(3-dimethylaminopropyl) carbodiimide (EDC) was obtained from Sigma-Aladdin Industrial Co., Ltd. Polyglycerol polyricinoleate (PGPR) and caprylic citrate triglyceride (GTCC) were purchased from Usoft Chemical Reagent Co., Ltd. Ethanol, hexane, dichloromethane, chloroform, triethylamine (TEA) were purchased from Sinopharm Chemical Reagent Co., Ltd. Fluo-4 AM ( $\text{Ca}^{2+}$  indicator), MQAE ( $\text{Cl}^-$  indicator) and 2,7-dichlorodihydrofluorescein diacetate (DCFH-DA) were obtained from Sigma-Aldrich. Anti-calcium pump PMCA4 ATPase antibody and Anti-TRPA1 antibody were purchased from Abcam. All reagents were used as received.

## Characterization

Scanning electron microscopy (SEM) images were taken by a scanning electron microscope (SU-70, Hitachi, Japan) and transmission electron microscopy (TEM) images were taken by a transmission electron microscope (HT7700, HITACHI, Japan). The energy dispersive spectroscopy (EDS) elemental mapping was obtained by a JEOL electron microscope (JEM-2100, JEOL, Japan). The phase identification was investigated by X-ray diffraction instrument (XRD, X'pert PRO MPD, Netherlands) with Cu K $\alpha$  radiation ( $\lambda = 0.154 \text{ nm}$ ) and operated at 40kV and 40mA. The UV-Vis absorption spectra were recorded by a UV-Vis spectrophotometer (UV2600, Shimadzu, Japan). The dynamic light scattering (DLS) size distribution was measured on a Malvern zetasizer (nano-ZS90, UK).

## Synthesis of KCCP NPs

Nanoparticles, consisting of potassium chloride nanocrystals and amorphous calcium carbonate (KCC NPs), were fabricated by a solvent evaporation method [1-2]. In brief, 2.47 g of calcium chloride dihydrate was dissolved into 10 mL of ethanol (solution A). 45 g of GTCC and 1.8 g of PGPR were mixed and stirred (solution B). Then, 0.5 mL of solution A was added into solution B. By stirring at 120 °C for 48 h, solutions were centrifuged and washed by hexane twice.

The  $\text{C}_{18}\text{PMH}$ -PEG was synthesized according to the previous study with modifications [3]. In brief, 10 mg  $\text{C}_{18}\text{PMH}$  and 286 mg mPEG-NH<sub>2</sub> were added into 5 mL  $\text{CH}_2\text{Cl}_2$ , and then 12  $\mu\text{L}$  TEA was added into the solution. After stirring for 24 h, 22 mg EDC and 22  $\mu\text{L}$  TEA were added into the solution prepared. After 24 h of stirring, the solution was blowing-dried by  $\text{N}_2$ . 10 mL water was added to dissolve the sample, and then the solution was dialyzed against distilled water for 48 h to remove unreacted mPEG-NH<sub>2</sub>. Finally, the  $\text{C}_{18}\text{PMH}$ -PEG was obtained by lyophilization and stored at -20°C for further use.

For the modification of KCC using PEG, 10 mg of prepared samples were dispersed into 1 mL of chloroform. Subsequently, 500  $\mu\text{L}$  of  $\text{C}_{18}\text{PMH}$ -PEG solution (1 mg/mL) was added into the solution, sonicated for 5 min and dried in  $\text{N}_2$  atmosphere. Finally,

the as-obtained PEG-modified KCC NPs were dispersed into water with concentration of 10 mg/mL for further use.

For the synthesis of Pt-integrated KCCP NPs (KCCP NPs) (Pt/KCC mass ratio of 5:100), 1.25 mg of  $K_2PtCl_6$  was added into the KCC solution. After stirring for 5 min, 12.5 mg of  $NaBH_4$  was dissolved in 1 mL of icy water, and  $NaBH_4$  solution was added into KCC solution. After 0.5 h reaction, KCCP NPs were obtained by centrifugation. KCCP-2 (Pt/KCC mass ratio of 2:100) and KCCP-1 (Pt/KCC mass ratio of 1:100) were synthesized in a similar way for comparison.

### Electro-catalytic properties

Methylene blue (MB), as a common ROS probe [4-5], was utilized to investigate electro-catalytic activity of as-prepared KCCP NPs. The experimental setup and parameter settings for the applied electric field were chosen according to the previous study. 50  $\mu$ L of MB (1 mM) was added into 2 mL of PBS, and different treatments were conducted (Ctrl, E (10mA, 10 mHz, square wave AC), KCCP (2 mg/mL for KCC and 100  $\mu$ g/mL for Pt) and KCCP + E). After different times, 50  $\mu$ L of solution was taken out and diluted four times. The absorption spectra of MB were investigated by UV-vis spectroscopy. Pt NPs in  $CaCl_2$  solutions with different concentrations were also studied. In addition, MB degradations of KCCP NPs with different ratios of platinum to KCC were studied. The platinum content in these KCCP NPs were kept the same to Pt NPs (100  $\mu$ g/mL). In addition, MB degradation of KCCP NPs with different ratios of platinum to KCC were also studied after 24 h pre-incubation in PBS.

### In vitro studies

$1 \times 10^4$  4T1 cells and AML-12 cells were planted in 96-well plate for 12 h, and different concentrations of  $K^+$ ,  $Cl^-$ ,  $Ca^{2+}$ , KCCP NPs and Pt NPs were added. The cell viabilities were evaluated by CCK-8 assay after incubation for 24 h.

$1 \times 10^5$  4T1 cells were seeded in 24-well plate and co-cultured with KCCP NPs and Pt NPs at varied concentrations for 4 h. Then, electric field (square wave, 10mHz, 5 mA) was imposed to the cells for 10 min. The cell viabilities were evaluated by CCK-8 assay after incubation for 24 h.

$1 \times 10^4$  4T1 cells were seeded in 96-well plate for 12 h. Then, PBS, KCCP (100  $\mu$ g/mL for KCC, 5  $\mu$ g/mL for Pt), Pt + E (5  $\mu$ g/mL, square wave, 10mHz, 5 mA, 10 min), Pt + E +  $Ca^{2+}$  (25.8  $\mu$ g/mL for  $Ca^{2+}$ ), Pt + E +  $Cl^-$  (17  $\mu$ g/mL for  $Cl^-$ ), KCCP + E (100  $\mu$ g/mL for KCC) were added and relative operations were conducted. The cell viabilities were evaluated by CCK-8 assay after incubation for 24 h.

To reveal the in vitro tumor inhibition mechanism of KCCP NPs, cells were treated with following protocols: (1) Ctrl; (2) electric field (E); (3) 0.8  $\mu$ M of A23187; (4) 8  $\mu$ M of BAPTA-AM; (5) 5 mM of NAC; (6) 5  $\mu$ g/mL of Pt NPs; (7) 5  $\mu$ g/mL of Pt NPs + E (square wave, 10 mHz, 5 mA, 10 min); (8) 0.8  $\mu$ M of A23187 and 5  $\mu$ g/mL of Pt NPs + E; (9) 8  $\mu$ M of BAPTA-AM and 5  $\mu$ g/mL of Pt NPs + E; (10) 5mM of NAC and 5  $\mu$ g/mL of Pt NPs + E; (11) KCCP NPs ([KCC]: 100  $\mu$ g/mL, [Pt]: 5  $\mu$ g/mL); (12) KCCP NPs ([KCC]: 100  $\mu$ g/mL, [Pt]: 5  $\mu$ g/mL) + E (square wave, 10mHz, 5 mA, 10 min); (13) 0.8  $\mu$ M of A23187 and KCCP NPs + E; (14) 8  $\mu$ M of BAPTA-AM and

KCCP NPs + E; (15) 5 mM of NAC and KCCP NPs + E. After culturing for another 24 h, the cell viabilities were analyzed by CCK-8 assay.

### **Measurement of intracellular chloride and calcium ion concentrations**

For the measurement of intracellular chloride ion, 4T1 cells were cultured with KCCP NPs (100 µg/mL for KCC, 5 µg/mL for Pt) for 0, 2, 4, 6 h. Then, 10 mM of MQAE was added and co-cultured for 30 min. The MQAE fluorescence was imaged by fluorescence microscope. Similar operations were conducted after cells incubated with KCCP NPs at varied concentrations (0, 12, 25, 50, 100 µg/mL for KCC, 0, 0.6, 1.25, 2.5, 5 µg/mL for Pt) for 6 h.

For the measurement of calcium ion, 4 µM of Fluo-4 AM was added and co-cultured for 30 min. The Fluo-4 AM fluorescence was imaged by fluorescence microscope.

### **Intracellular ROS generation**

After different treatments (PBS, E (10mHz, 5mA, 10 min), Pt (5 µg/mL) + E and Pt + E + Cl<sup>-</sup> (17 µg/mL for Cl<sup>-</sup>)), 4T1 cells were stained with 20 µM of DCFH-DA and 1 µg/mL of DAPI. The fluorescence images were obtained by fluorescence microscope. After different treatments (PBS, E (10mHz, 5mA, 10 min), KCCP ([KCC]: 100 µg/mL, [Pt]: 5 µg/mL), Pt (5 µg/mL) + E, KCCP + E, KCCP + E + BAPTA (8 µM) and KCCP + E + A23187 (0.8 µM)), 4T1 cells were stained with 20 µM of DCFH-DA and 1 µg/mL of DAPI. The fluorescence images were obtained by fluorescence microscope.

### **Western Blot Assay**

Different groups were co-cultured with 4T1 cells for 4 h and square-wave AC electric field (10mHz, 5mA, 10 min) was applied to cells. After 12 h, 200 µL of lysis buffer was added and the solution was centrifuged. Then, the SDS buffer was added into the supernatant and boiled for 5 min. Next, 12% SDS-PAGE was used to separate the samples. After transferring to the PVDF membrane, the samples were co-cultured with anti-calcium pump PMCA4 ATPase antibody, anti-TRPA1 antibody and anti-actin antibody overnight at 4 °C. Subsequently, the samples were cultured with a secondary antibody for 1h. Finally, Bio-Rad chemoluminescence imaging system was used to measure the bands.

### **In vivo study**

Four-week-old female Balb/c mice were purchased from Shanghai Slac Laboratory Animal Co. Ltd. and used in compliance with guidelines of the Biological Resource Centre of the Agency for Science, Technology and Research, Zhejiang University. 4T1 cells was injected to the mice for animal experiments. The animal experiments were grouped as follows: (1) control; (2) E; (3) KCCP ([KCC]: 4 mg/mL, [Pt]: 0.2 mg/mL, 50 µL); (4) Pt (0.2 mg/mL for Pt, 50 µL) + E (square wave, 10 mHz, 5 mA, 10 min); (5) KCCP ([KCC]: 4 mg/mL, [Pt]: 0.2 mg/mL, 50 µL) + E (square wave, 10 mHz, 5 mA, 10 min). After the nanoparticles were intratumorally injected into the mice for 10 min, the square wave AC field (5 mA, 10 min) was applied to the mice in groups of E, Pt + E and KCCP + E. Then, the tumor sizes were measured every two days.

## Reference

- [1] J.P. Paques, E. van der Linden, L.M.C. Sagis et al., *J. Agric. Food Chem.*, 2012, **60**, 8501-8509.
- [2] H. Lin, Z. Lei, Z. Jiang et al., *J. Am. Chem. Soc.*, 2013, **135**, 9311-9314.
- [3] Liang Cheng , Weiwei He , Hua Gong et al., *Adv. Funct. Mater.*, 2013, **23**, 5893-5902.
- [4] J. S. Lee, K.H. You, C.B. Park, *Adv. Mater.*, 2012, **24**, 1084-1088.
- [5] Y. Tang, W. Di, X. Zhai et al., *ACS Catal.*, 2013, **3**, 405-412.

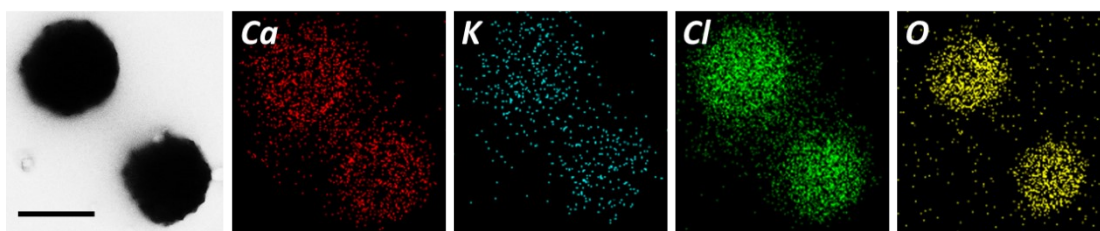


**Fig. S1** The EDS element mapping image of KCC nanoparticles (scale bar = 500 nm).

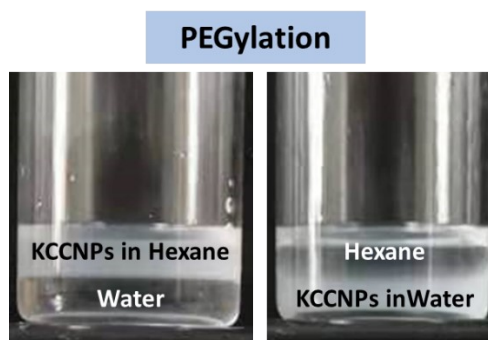


**Fig. S2** Photographs of KCC NPs in the mixture of hexane and water before and after PEG modification.

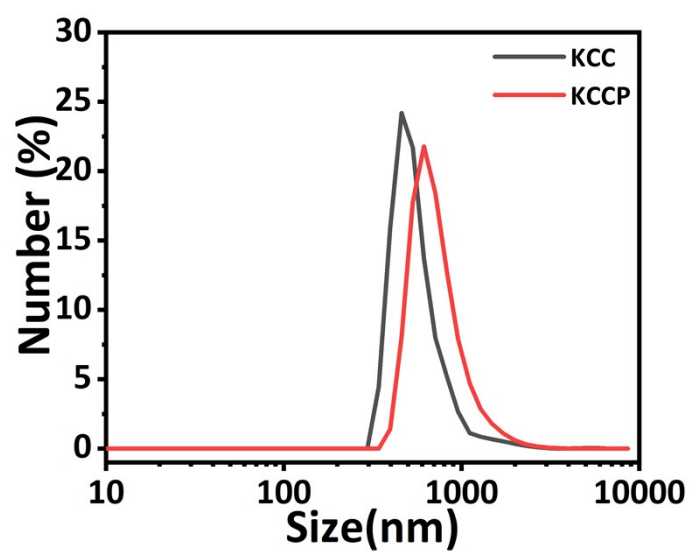


**Fig. S3** The hydrodynamic size distribution of KCC NPs and KCCP NP.

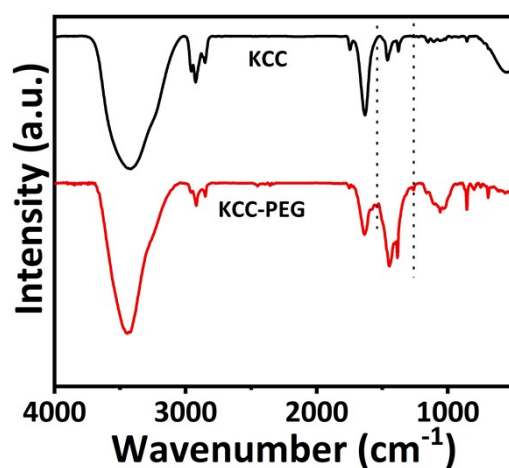


**Fig. S4** Fourier transformed infrared (FTIR) spectra of KCC nanoparticles with or without C<sub>18</sub>PMH-PEG modification.

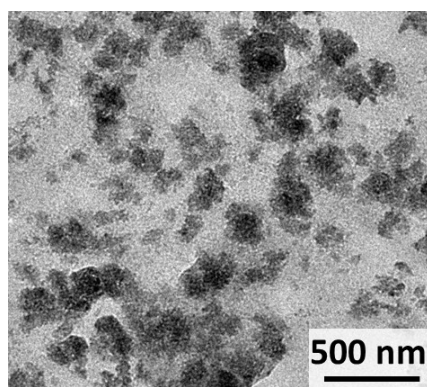


**Fig. S5** TEM image of KCCP NPs after incubated in water for 24 h.

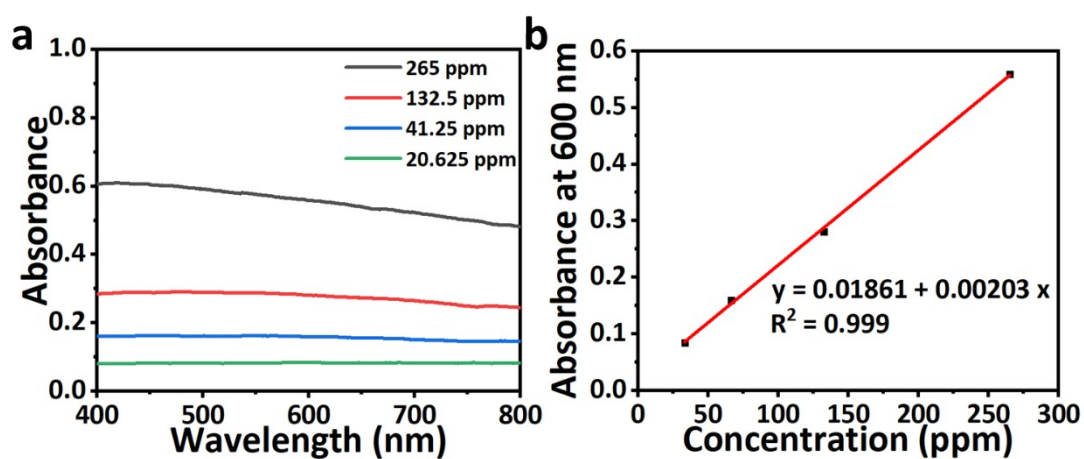


**Fig. S6** (a) UV-vis absorption spectra of KCC solutions with different concentrations, and (b) the relationship between the optical absorbance at 600 nm and the concentration of KCC solutions.

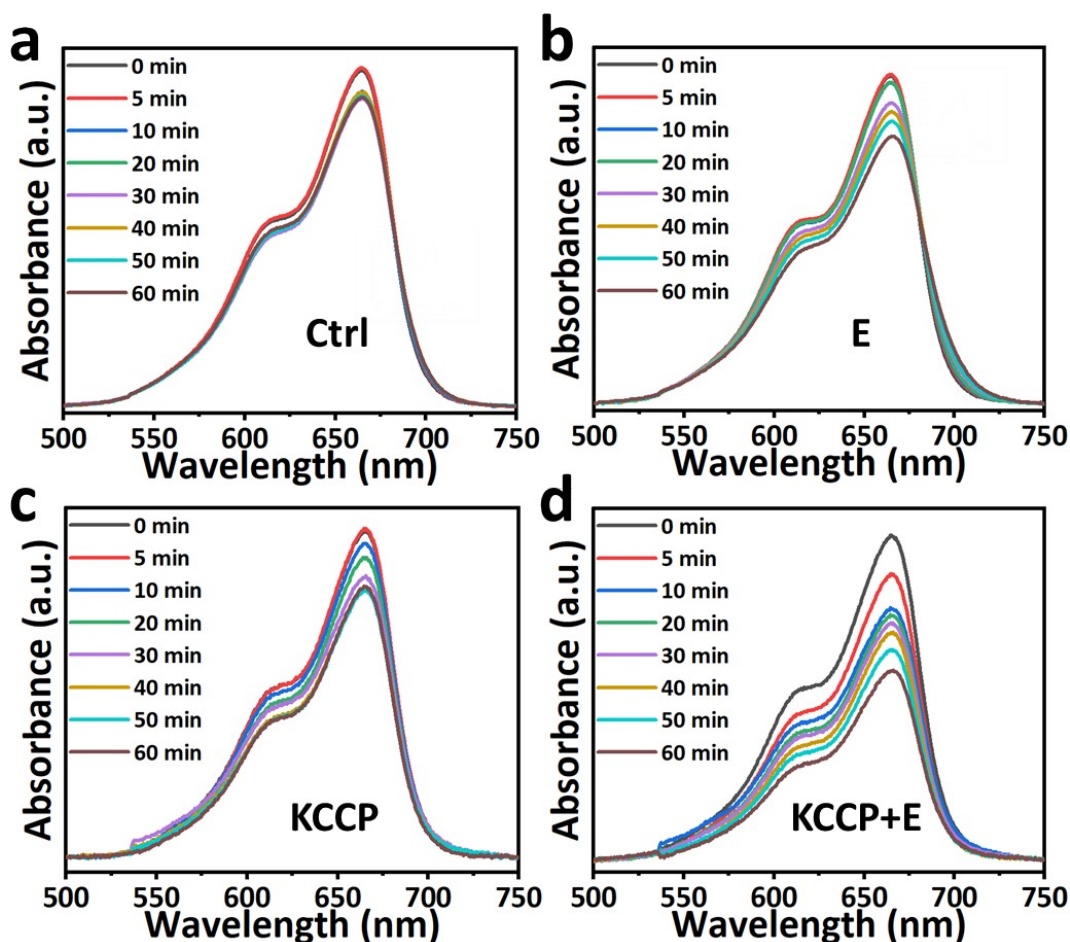


**Fig. S7** UV-vis absorption spectra of MB solutions under different conditions: (a) PBS, (b) electric field, (c) KCCP NPs, (d) KCCP under electric field. ([KCC]:  $2 \text{ mg mL}^{-1}$ , [Pt]:  $100 \text{ } \mu\text{g mL}^{-1}$ , AC output current: 10 mHz, 10mA, [MB]:  $2.5 \times 10^{-5} \text{ M}$ ).

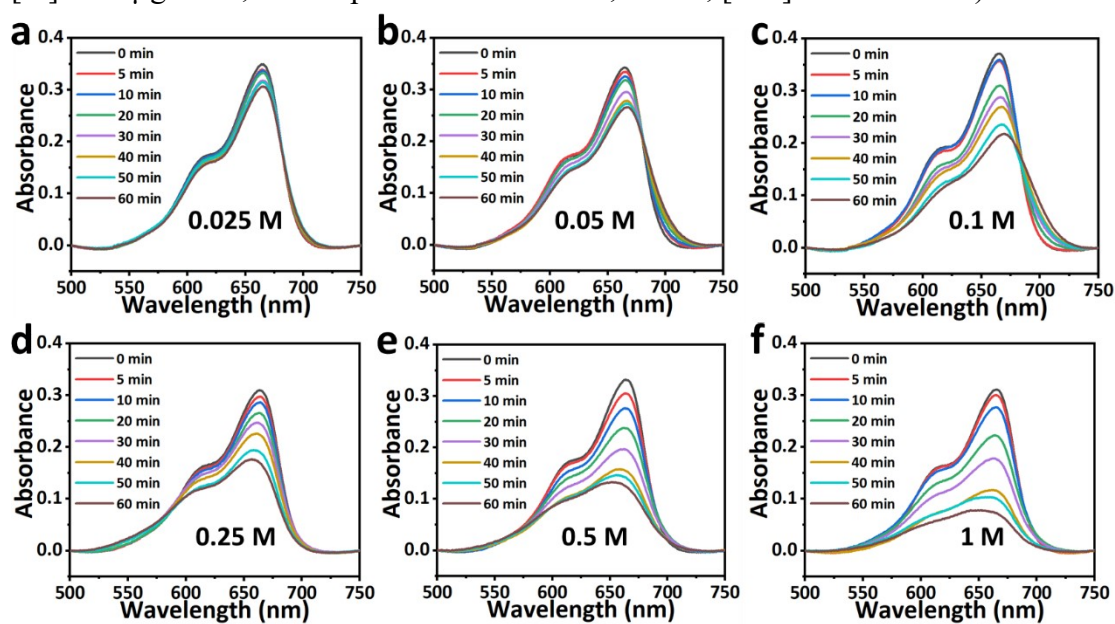


**Fig. S8** UV-vis absorption spectra of MB degraded by Pt NPs in different concentrations of  $\text{CaCl}_2$  solutions (a) 0.025 M, (b) 0.05 M, (c) 0.1 M, (d) 0.25 M, (e) 0.5 M and (f) 1 M (AC output current: 10 mHz, 10mA, [MB]:  $2.5 \times 10^{-5} \text{ M}$ ).



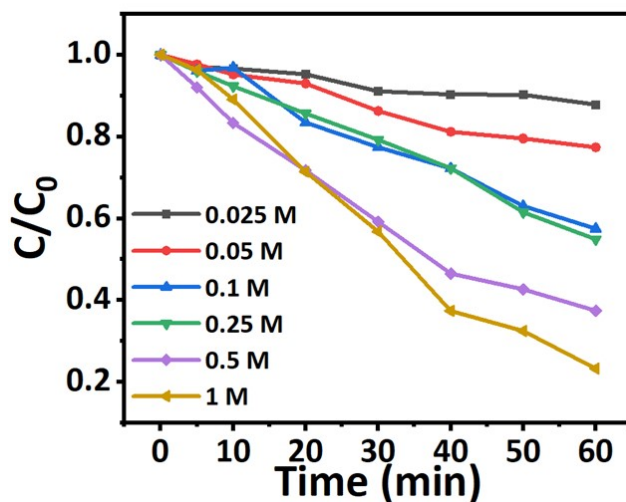


**Fig. S9** MB degradation properties by Pt NPs with different concentrations of chloride ion under electric field.

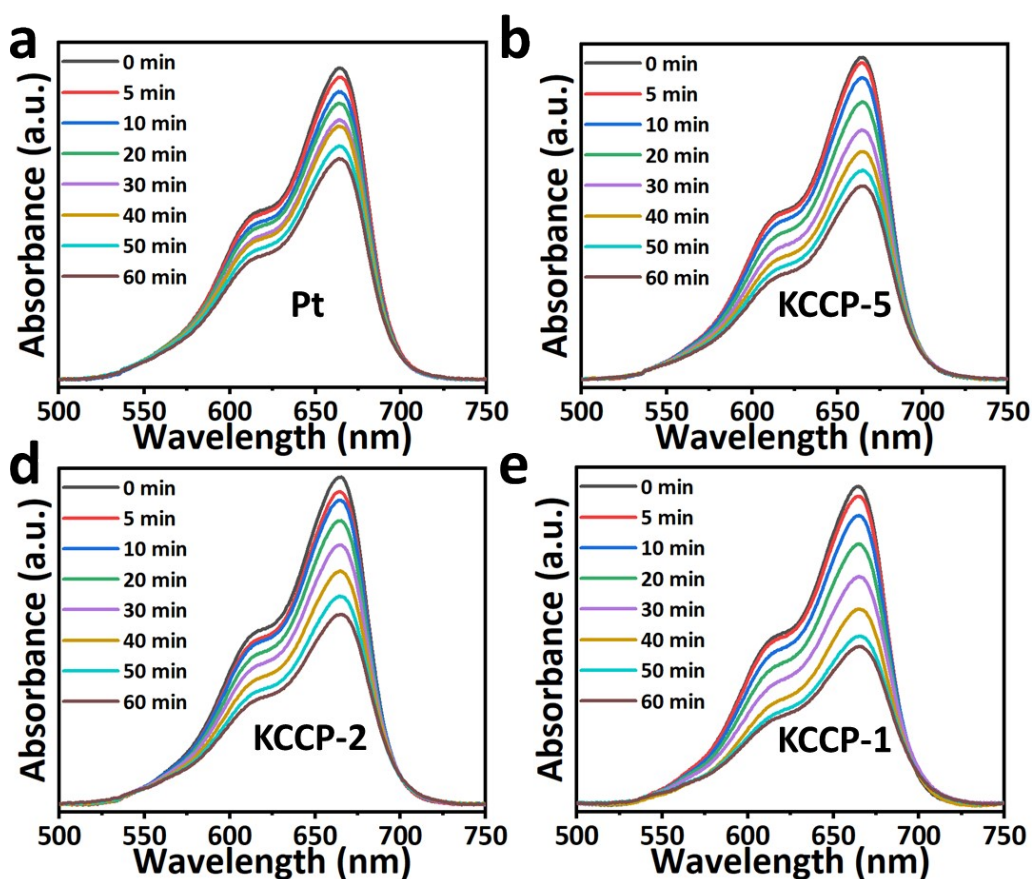


**Fig. S10** UV-vis absorption spectra of MB solutions degraded by different KCCP NPs under electric field: (a) Pt, (b) KCCP-5, (c) KCCP-2 and (d) KCCP-1 (AC output current: 10 mHz, 10mA, [MB]:  $2.5 \times 10^{-5}$  M).

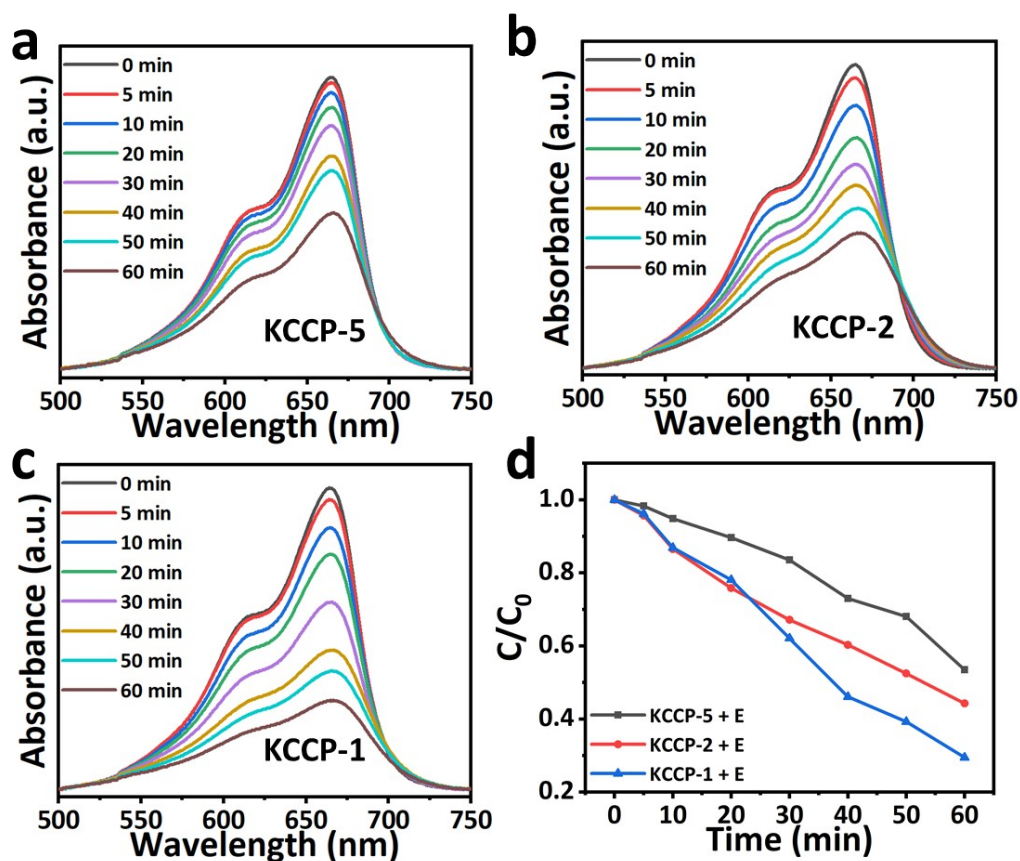


**Fig. S11** UV-vis absorption spectra of MB solutions degraded by different KCCP NPs under electric field after 24 h pre-incubation: (a) KCCP-5 (b) KCCP-2 and (c) KCCP-1 (AC output current: 10 mHz, 10mA, [MB]:  $2.5 \times 10^{-5}$  M). (d) MB degradation properties by different KCCP NPs under electric field after 24 h pre-incubation in PBS.

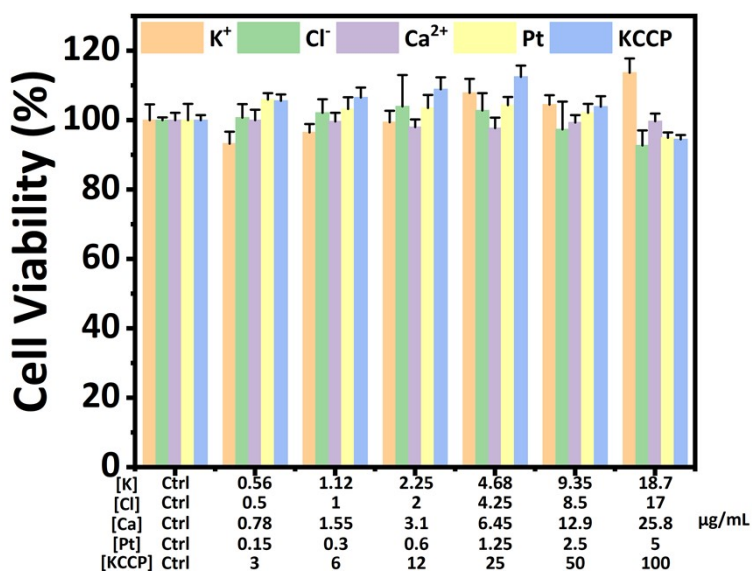


**Fig. S12** The viabilities of AML-12 cell cultured with K<sup>+</sup>, Cl<sup>-</sup>, Ca<sup>2+</sup>, Pt NPs and KCCP NPs.

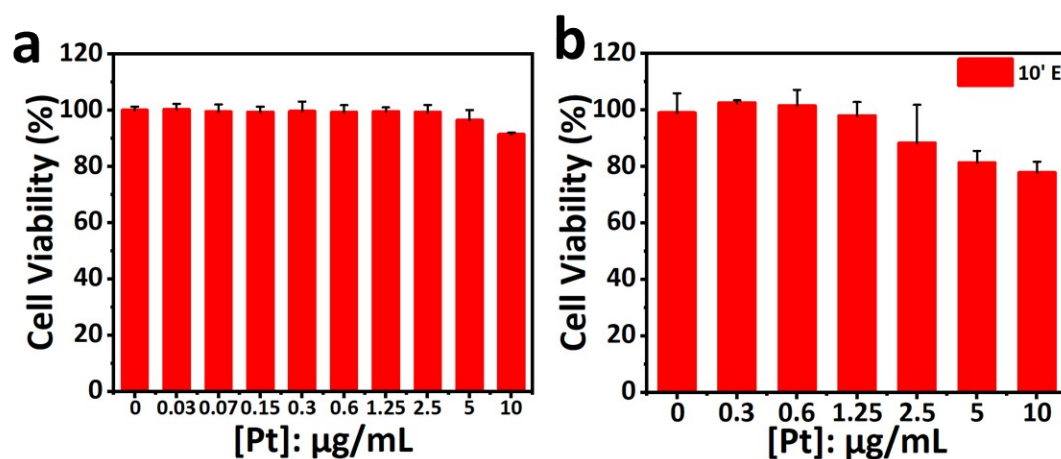


**Fig. S13** (a) 4T1 cell viabilities after cultured with Pt NPs. (b) 4T1 cell viabilities after cultured with Pt NPs under electric field.

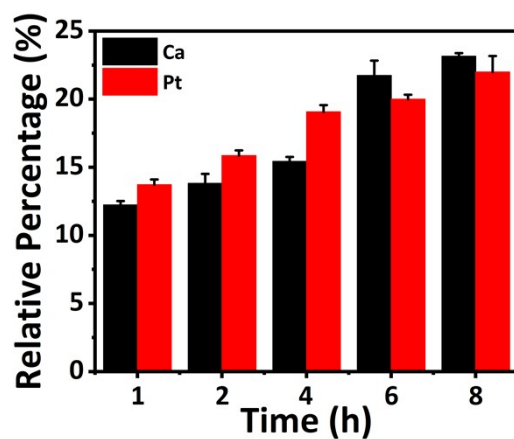


**Fig. S14** ICP analysis of 4T1 cells incubated with KCCP for different time.

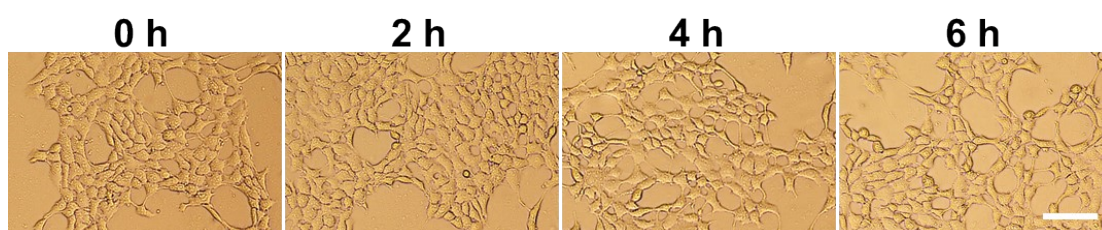


**Fig. S15** The bright field images of cells treated with KCCP NPs after different times for intracellular  $\text{Cl}^-$  ion detection (scale bar = 100  $\mu\text{m}$ ).

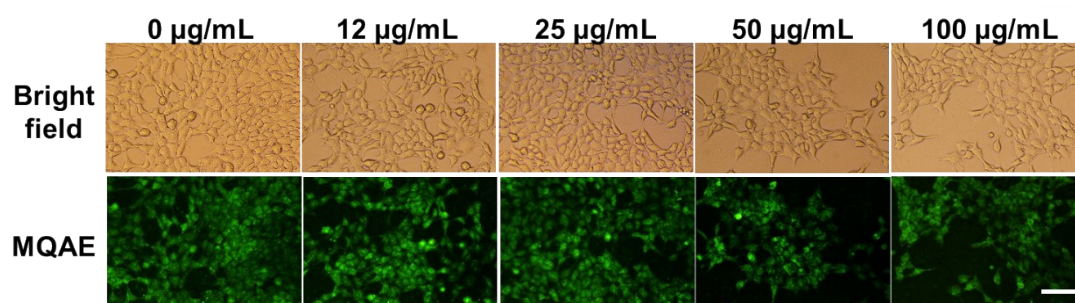


**Fig. S16** Intracellular  $\text{Cl}^-$  concentration after incubated with different concentrations of KCCP NPs using MQAE as probe (scale bar = 100  $\mu\text{m}$ ).

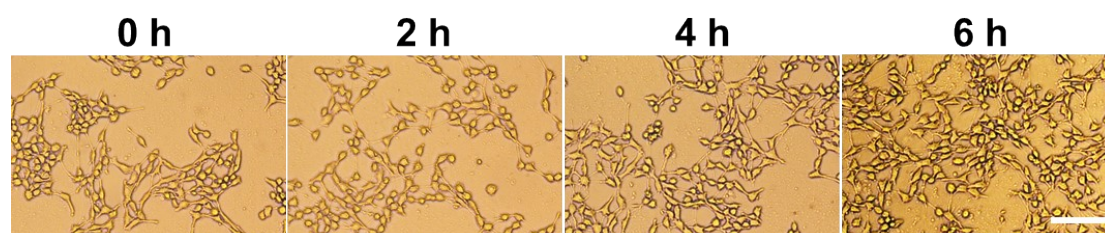


**Fig. S17** The bright field images of cells treated with KCCP NPs after different times for intracellular  $\text{Ca}^{2+}$  ion detection (scale bar = 100  $\mu\text{m}$ ).

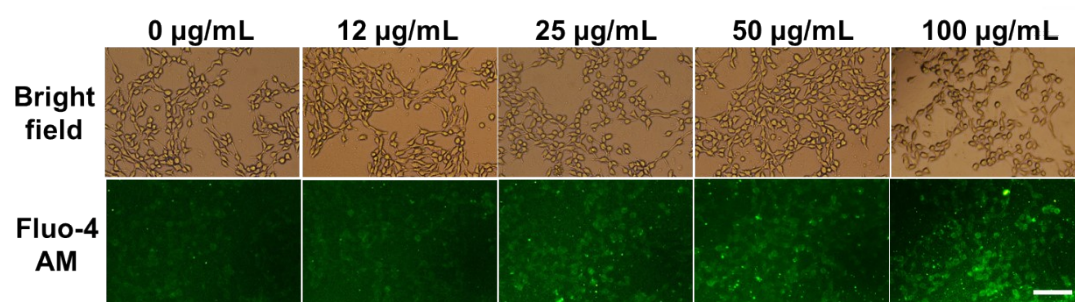


**Fig. S18** Intracellular  $\text{Ca}^{2+}$  concentration after incubated with different concentrations of KCCP NPs using Fluo-4 AM as probe (scale bar = 100  $\mu\text{m}$ ).



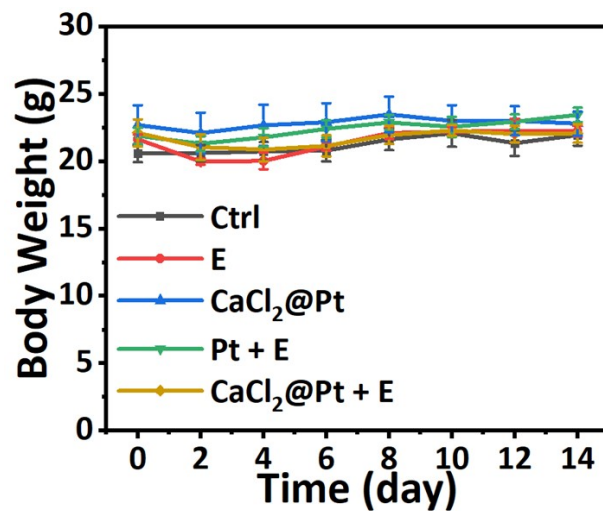


**Fig. S19** The average body weights of mice after different treatments.

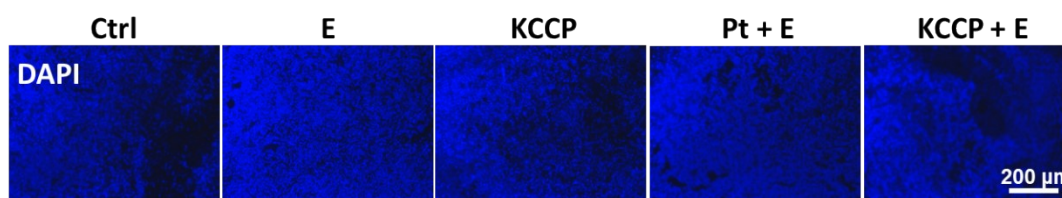


**Fig. S20** Fluorescence images of DAPI-stained tumor slices after different treatments (scale bar = 100  $\mu$ m).